Cdc1 removes the ethanolamine phosphate of the first mannose of GPI anchors and thereby facilitates the integration of GPI proteins into the yeast cell wall

Hector M. Vazquez, Christine Vionnet, Carole Roubaty, and Andreas Conzelmann
Department of Biology, University of Fribourg, CH-1700 Fribourg, Switzerland

ABSTRACT **Temperature-sensitive *cdc1^{ts}* mutants are reported to stop the cell cycle upon a shift to 30°C in early G2, that is, as small budded cells having completed DNA replication but unable to duplicate the spindle pole body. A recent report showed that PGAP5, a human homologue of *CDC1*, acts as a phosphodiesterase removing an ethanolamine phosphate (EtN-P) from mannose 2 of the glycosylphosphatidylinositol (GPI) anchor, thus permitting efficient endoplasmic reticulum (ER)-to-Golgi transport of GPI proteins. We find that the essential *CDC1* gene can be deleted in *mcd4*Δ cells, which do not attach EtN-P to mannose 1 of the GPI anchor, suggesting that Cdc1 removes the EtN-P added by Mcd4. *Cdc1-314^{ts}* mutants do not accumulate GPI proteins in the ER but have a partial secretion block later in the secretory pathway. Growth tests and the genetic interaction profile of *cdc1-314^{ts}* pinpoint a distinct cell wall defect. Osmotic support restores GPI protein secretion and actin polarization but not growth. Cell walls of *cdc1-314^{ts}* mutants contain large amounts of GPI proteins that are easily released by β-glucanases and not attached to cell wall β1,6-glucans and that retain their original GPI anchor lipid. This suggests that the presumed transglycosidases Dfg5 and Dcw1 of *cdc1-314^{ts}* transfer GPI proteins to cell wall β1,6-glucans inefficiently.**

Monitoring Editor
Akihiko Nakano
RIKEN

Received: Jun 3, 2014
Revised: Jul 25, 2014
Accepted: Aug 18, 2014

INTRODUCTION

Glycosylphosphatidylinositol (GPI) anchoring in yeast and mammals

In all eukaryotes GPI lipids are posttranslationally attached to the C-terminus of certain proteins in the lumen of the endoplasmic reticulum (ER). Genetic ablation of GPI anchoring leads to embryonic lethality in humans and lethality in yeast (Maeda and Kinoshita, 2011). While all GPI proteins in mammals are exposed at the plasma membrane, only about half of yeast GPI proteins stay in the plasma membrane; the other half loses the GPI lipid moiety and gets covalently attached to the cell wall β1,6-glucans (Caro *et al.*, 1997; Hamada *et al.*, 1998; de Groot *et al.*, 2003). Indeed, among the yeast cell wall proteins (CWPs) that are covalently attached to β-glucans, the majority are initially GPI anchored (GPI-CWPs), whereas a minority are linked via an alkali-sensitive linkage to β1,3-glucans (ASL-CWPs) (de Groot *et al.*, 2005).

The activity transferring GPI proteins from the plasma membrane onto β-glucans may reside with Dfg5 and Dcw1, two highly homologous GPI proteins (54% identity; Kitagaki *et al.*, 2002). During the transfer of GPI-CWPs to cell wall glucans, the glucosamine–inositol–phospholipid moiety of the anchor is lost, whereas four to five mannoses (Man), the phosphodiester bond, and the bridging ethanolamine (EtN) remain attached to the protein (Figure 1). Therefore Dfg5 and Dcw1, having homology with bacterial endomannosidases, are proposed to cleave the Manα1,4glucosamine linkage of the GPI anchor and to reattach the liberated Man residue with the attached GPI protein to β1,6-glucans of the cell wall (Kollar *et al.*, 1997; Fujii *et al.*, 1999; Kitagaki *et al.*, 2002). Simultaneous

This article was published online ahead of print in MBoC in Press (http://www.molbiolcell.org/cgi/doi/10.1091/mbc.E14-06-1033) on August 27, 2014.

Address correspondence to: Andreas Conzelmann (andreas.conzelmann@unifr.ch).

Abbreviations used: ASL-CWP, alkali-sensitively–linked cell wall protein; CFW, calcofluor white; CWP, cell wall protein; DTT, dithiothreitol; ER, endoplasmic reticulum; EtN, ethanolamine; EtN-P, EtN-phosphate; GFP, green fluorescent protein; GPI, glycosylphosphatidylinositol; GPI-CWP, GPI-anchored cell wall protein; HA, hemagglutinin; IPC, inositol phosphorylceramide; Man, mannose; MW, molecular weight; PI, phosphatidylinositol; SC, synthetic complete; SGA, synthetic genetic array; ts, temperature sensitive; UPR, unfolded protein response; YPD, yeast–peptone–dextrose; WT, wild type.

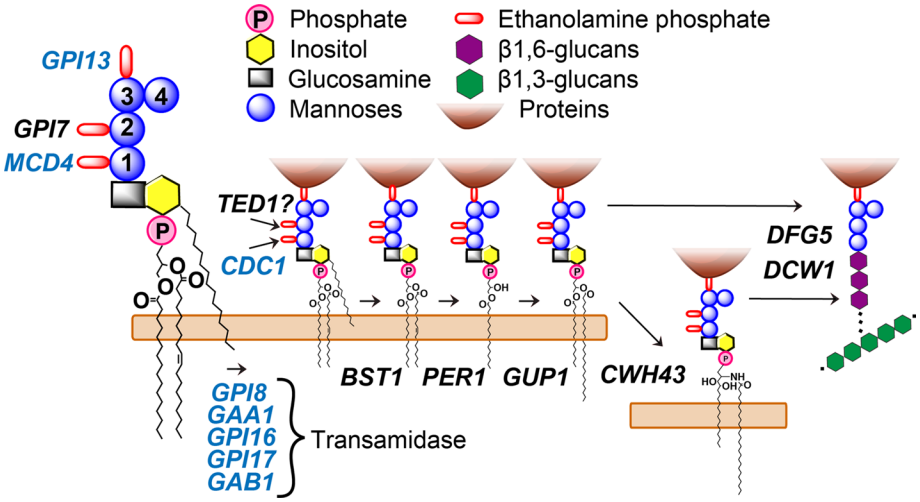

FIGURE 1: GPI anchor remodeling and subsequent attachment to the cell wall. Essential genes are indicated in blue. Mature GPI anchor lipids (left) contain EtN-Ps on Man1, Man2, and Man3; their addition is catalyzed by *MCD4*, *GPI7*, and *GPI13*, respectively. After the protein is attached to the GPI lipid by the transamidase complex, the lipid moiety is remodeled by Bst1, Per1, Gup1, and Cwh43 (middle). At some time during lipid remodeling, EtN-Ps may be removed from Man1 and Man2. At the plasma membrane, Man1 of the anchor of GPI-CWPs is transferred and covalently linked to β1,6-glucans. This reaction is presumably catalyzed by Dcw1 and Dfg5.

deletion of *DFG5* and *DCW1* is lethal, suggesting that the covalent attachment of GPI-CWPs to glucans is essential, and this remains true even if cells receive osmotic support (Kitagaki *et al.*, 2002).

GPI lipid remodeling in yeast

GPI lipids in yeast and mammals are constructed in the ER by sequential addition of sugars to a phosphatidylinositol (PI) and then are attached to proteins, the entire process requiring more than 20 genes. The GPI lipid usually contains C16:0 and C18:1 fatty acids (Pittet and Conzelmann, 2007; Fujita and Jigami, 2008). After attachment of the GPI lipid to yeast GPI proteins, the lipid moiety is remodeled so as to contain a C26:0 fatty acid rather than C18:1 or a phytosphingosine-C26:0–type ceramide. Ceramide anchors are also found in the GPI anchors of other fungi, certain plants, *Dictyostelium*, and protozoan organisms (Fankhauser *et al.*, 1993; Pittet and Conzelmann, 2007; Fujita and Jigami, 2008). These remodeling reactions occur in the ER and are a prerequisite for the concentration of GPI proteins in the ER exit sites (Castillon *et al.*, 2009, 2011).

By composition, yeast GPI anchors of detergent-extractable GPI proteins and GPI anchor remnants of GPI proteins linked to cell wall β-glucans did not contain EtN-phosphate (EtN-P) side chains on Man1 and Man2 (Figure 1; Fankhauser *et al.*, 1993; Fujii *et al.*, 1999). While such residues may have been lost during purification, these reports are certainly compatible with the idea that EtN-P side chains are removed during maturation of GPI proteins. Yeast *CDC1* and *TED1* show 21 and 23% identities to 73 and 39% of PGAP5 sequence, respectively, and *TED1* shows 23% identity to 33% of *CDC1* sequence. Moreover, *ted1*Δ mutants show a similar GPI protein transport defect as PGAP5 mutants (Haass *et al.*, 2007). Thus *CDC1* and *TED1* are candidates for enzymes removing EtN-P side chains.

Discovery of *CDC1*

CDC1 is an essential gene. Temperature sensitive (ts) *cdc1*^{ts} alleles were identified as cell cycle mutants accumulating upon a shift to nonpermissive temperature as cells with no or only a small bud, mostly duplicated DNA, a nonduplicated spindle pole body, and an undivided nucleus (Paidhungat and Garrett, 1998b). Subsequent work revealed that certain *cdc1*^{ts} alleles are rescued by supplementing media with Mn^{2+} or overexpression of plasma membrane Mn^{2+} transporters Smf1 or Smf2. Moreover, even wild-type (WT) cells, when deprived of Mn^{2+}, stop cycling and exhibit small buds, duplicated DNA, and an undivided nucleus (Loukin and Kung, 1995; Supek *et al.*, 1996; Eguez *et al.*, 2004). These data led to the proposal that Cdc1 regulates the Mn^{2+} concentrations in cells, and this view was supported by the finding that deletion of *PER1*, now known to remove the sn2-linked fatty acid of the primary GPI anchor (Figure 1), allows for the deletion of *CDC1* as long as Mn^{2+} is present in high concentrations in the media (Paidhungat and Garrett, 1998a).

A more recent study found strong evidence that Cdc1 is not regulating but is regulated by the intracellular Mn^{2+} concentration and that it is a Mn^{2+}-dependent phosphodiesterase. Indeed, mutation of amino acids belonging to the Mn^{2+}-binding motif caused a Cdc1-deficiency phenotype (Losev *et al.*, 2008). These studies also showed that many *cdc1*^{ts} cells at 30°C have an elevated Ca^{2+} content and that elevated cytosolic Ca^{2+} levels contribute to the growth phenotype, to actin depolarization, and, related to this, a Golgi inheritance defect, whereby these phenomena are suppressed upon deletion of plasma membrane calcium channel components Mid1 or Cch1 (Paidhungat and Garrett, 1997; Rossanese *et al.*, 2001; Losev *et al.*, 2008). However, abolition of the calcium channel did not allow growth of *cdc1*^{ts} cells at 37°C.

The above-mentioned GPI anchor modification function of the mammalian homologue PGAP5 drove us to investigate the effect of *cdc1* mutants on GPI protein biosynthesis in yeast.

RESULTS

Does Cdc1 remove an EtN-P from either Man1 or Man2?

EtN-P is added to Man1, Man2, and Man3 of the GPI lipid precursor by Mcd4, Gpi7, and Gpi13, respectively (Figure 1). Among these three paralogues, only *GPI7* is not essential. Previous data indicated that *ted1*Δ mutants retain the GPI protein Gas1 in the ER and that *gpi7*Δ and *ted1*Δ each induce a strong unfolded protein response (UPR), which does not get stronger in a *gpi7*Δ/*ted1*Δ double mutant (Jonikas *et al.*, 2009). This mutual phenotypic suppression but absence of correlation of the phenotypic interaction profiles of *ted1*Δ and *gpi7*Δ raises the possibility that Ted1 removes the EtN-P from Man2, explaining why the UPRs of *ted1*Δ and *gpi7*Δ are not aggravating each other. This paradigm suggests that the lack of a EtN-P phosphodiesterase may be compensated by the lack of the EtN-P transferase adding the EtN-P that cannot be removed.

We did not find any negative genetic interaction of the temperature-sensitive *cdc1-314* allele with *gpi7*Δ (see Supplemental Table S1) nor is such an interaction recorded in BioGRID (http://thebiogrid.org). Thus the genetic data do not indicate that Cdc1 would have the same function as Ted1.

To investigate whether Cdc1 may be involved in the removal of EtN-P from Man1, we produced a *cdc1*Δ/*mcd4*Δ haploid strain

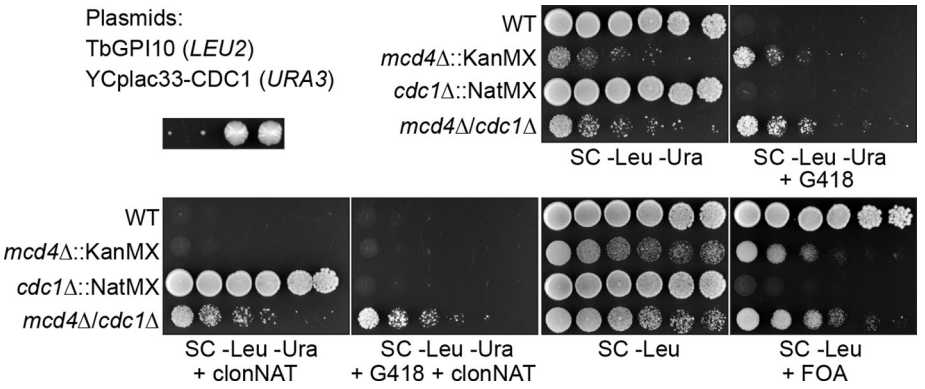

FIGURE 2: The essential *CDC1* gene can be deleted in the *mcd4*Δ mutant, which fails to add EtN-P onto Man1 of the GPI anchor. A diploid *mcd4*Δ*/MCD4 cdc1*Δ*/CDC1* strain harboring vectors expressing GPI10 from *Trypanosoma brucei* (TbGPI10) (*LEU2*) and yeast *CDC1* (*URA3*) was sporulated and dissected. A tetratype tetrad is shown at the top left; haploid offspring carrying *mcd4*Δ are producing very small colonies. The four colonies of this tetrad were grown, and 10-fold dilutions of cells were spotted on SC media with indicated supplements and grown at 30°C for 2–3 d.

harboring two different plasmids carrying yeast *CDC1* and TbGPI10. *MCD4* is an essential gene, because Gpi10, the mannosyltransferase adding Man3, does not work on GPI lipid intermediates lacking EtN-P on Man1, but *MCD4* becomes nonessential if yeast harbors the *GPI10* orthologue from *Trypanosoma brucei*, a species that does not add EtN-P onto Man1 (Zhu *et al.*, 2006). *Mcd4*Δ cells have dividing times three times longer than WT in liquid media and also grow badly on plates (Zhu *et al.*, 2006). As shown in Figure 2, *cdc1*Δ harboring TbGpi10 is unable to grow but *mcd4*Δ*/cdc1*Δ harboring TbGpi10 grows as fast as *mcd4*Δ harboring TbGpi10. This indicates that deletion of *CDC1* in a *mcd4*Δ background has no negative growth effect and our data (see Figure 6A, rows *mcd4*Δ and *mcd4*Δ*/cdc1*, later in this article) show that it does not aggravate the cell wall defect of *mcd4*Δ. Thus, whatever the problem caused by the deletion of the essential *CDC1* gene may be, it is fully compensated by not adding EtN-P to Man1 during the biosynthesis of the GPI lipid precursor. This constellation strongly suggests that Cdc1 has specialized in removing EtN-P from Man1.

Genetic interactions of *cdc1*

We sought to better understand the function of Cdc1 by doing a systematic genetic array (SGA) study to find other mutations that would modulate the growth of a well-characterized temperature-sensitive *cdc1-314* allele that was found to have a rather normal affinity for its essential cofactor Mn^{2+} but showed strong Ca^{2+} accumulation and an actin depolarization defect at 33.5°C (Losev *et al.*, 2008). In the rest of this paper, ordinary strains containing this allele will be referred to as *cdc1* and query strains for SGA will be referred to as *cdc1**.

As shown in Figure 3A, *cdc1** was unable to grow at 30°C; its growth was restored by WT *CDC1*, but not *cdc1*^{D144A}, which has a point mutation in the Mn^{2+}-binding motif (Losev *et al.*, 2008). The *CDC1** and *cdc1** (*cdc1-314*) query strains were both crossed in quadruplicate to a library of 5850 mutants comprising deletions for each of the nonessential genes and 879 DAmP alleles of essential genes (Breslow *et al.*, 2008).

Screens were done in parallel at 24, 26, and 30°C to detect synthetic sick interactions at permissive (24°C) and semipermissive (26°C) temperatures and suppressors at nonpermissive (30°C) temperature. Typical examples of such interactions are seen in the colored boxes of Figure 3B. The scores of the interactions retained after a first filtering (see *Materials and Methods*) had a normal distribution, and more negative than positive significant interactions were found (Figure 3C, colored dots). A complete list of the strains used in the SGA screen and of significant interactions ($p < 0.01$) is given in Supplemental Table S1.

Significant hits were manually attributed to functional categories, as shown in Figure 3, D–F, and Table S2. Among negative interactors (Figure 3, D and E), significant enrichments were found in genes orchestrating cell wall biosynthesis, ER protein folding, N-glycosylation, antero- and retrograde transport between ER and Golgi, and vacuolar H^+-ATPase assembly. The latter may score because cytosolic calcium levels are regulated in part by the vacuolar cation/H^+-exchanger Vcx1. Indeed, deletions in the plasma membrane calcium channel components Mid1 or Cch1 were shown to rescue growth of *cdc1-1* at 30°C on yeast–peptone–dextrose (YPD) medium (Paidhungat and Garrett, 1997; Losev *et al.*, 2008), but our screen did not pick up these suppressors, possibly because the Ca^{2+} concentration in synthetic complete (SC) medium used here is sixfold higher than in YPD. Interestingly, a strong negative genetic interaction of *cdc1* with *cnb1*Δ, deleting the obligatory regulatory subunit of the calcium-dependent protein phosphatase calcineurin, was seen in our screen and also noted in a previous report (Paidhungat and Garrett, 1997). It suggests that the elevation of cytosolic Ca^{2+} may also have a positive effect of unknown nature. This positive effect is not mediated by the calcineurin-dependent transcription factor Crz1, because *crz1*Δ had no negative effect on the growth of *cdc1* (Table S1).

Also, the Mn^{2+} and metal-ion transporters Smf1 and Smf2 of the plasma membrane were identified as negative interactors, suggesting that *cdc1-314*^{ts} may still be somewhat sensitive to Mn^{2+} depletion (Losev *et al.*, 2008). At 26°C, genes affecting ribosomal protein production also were enriched (Figure 3F). It is conceivable that the response to loss of Cdc1 function involves active protein synthesis.

The 22 deletions rescuing growth at 30°C mostly fell into one of three classes: the ER-associated protein degradation (ERAD) pathway, ER-to-Golgi transport, and GPI remodeling. In the latter category fell *gup1*Δ and *per1*Δ, which had previously been identified as suppressors of the growth defect of *cdc1*^{ts} mutants (Paidhungat and Garrett, 1998a). Some of the suppressor mutants were tested also by serial dilution assays, and all of them were found to enhance growth of *cdc1* in serial dilution growth assays, as shown in Supplemental Figure S1.

In summary, the screen suggested several biological processes that either aggravate or mitigate the effects of the *cdc1-314*^{ts} mutation, the effects of which we explored further as described in the following sections.

Stability of Cdc1-314 and Cdc1 proteins

Because ERAD mutants rescued growth of *cdc1* (Figure 3F), we hypothesized that ERAD mutants may stabilize Cdc1-314. To verify this, we expressed HA-Cdc1 or HA-Cdc1-314, that is, tagged versions carrying the hemagglutinin-derived HA epitope (HA) under the native promoter from a centromeric vector in WT cells and quantified the amounts of HA-tagged protein after shifting cells from 24° to 30° or 37°C, as shown in Figure 4A. In cells growing at 24°C, Cdc1-314 already was 3.8-fold less abundant than WT Cdc1. A shift

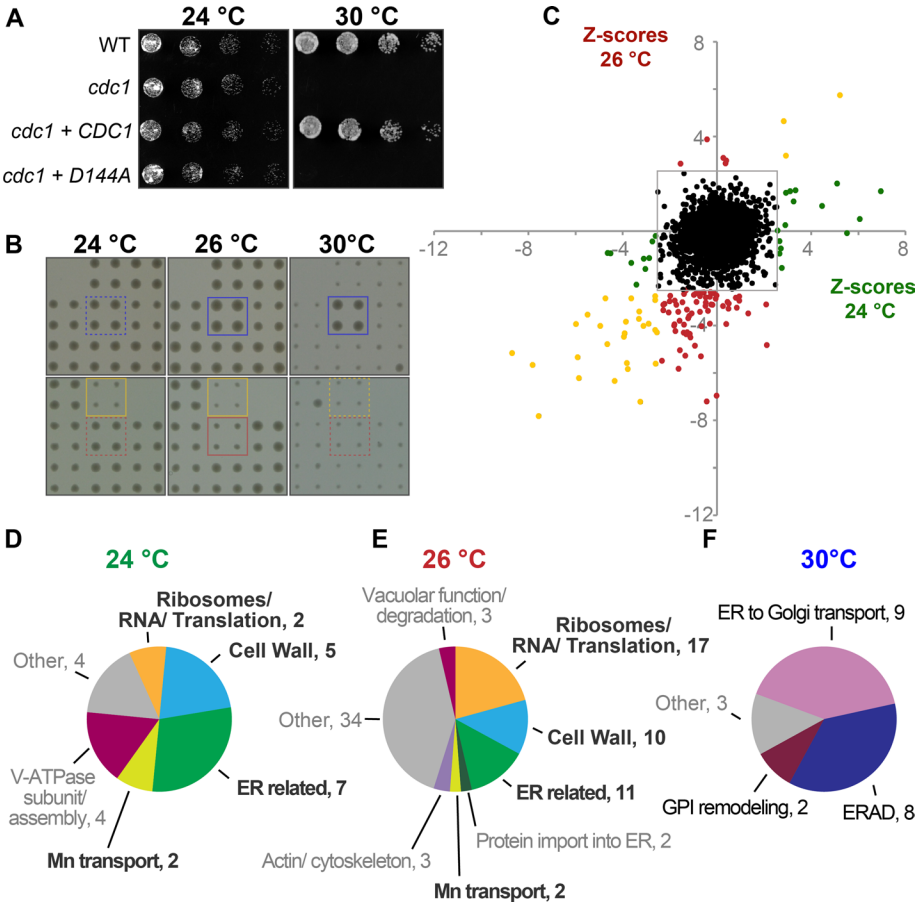

FIGURE 3: Genetic interactions of *cdc1*. (A) Fourfold dilutions of *cdc1*, *cdc1* harboring WT *CDC1*, or the functionally dead *cdc1*^{D144A} allele were incubated at 24 or 30°C. (B) Small areas from plates used to obtain colony sizes and *Z*-scores for *cdc1/geneX*Δ double mutants are shown. The upper three and lower three areas each show the same mutants selected either at 24, 26, or 30°C. Two double mutants (in quadruplicate) showing significant negative interaction at 24 as well as 26°C, or only at 26°C, are boxed in yellow and red, respectively, one showing positive genetic interaction is boxed in blue. The same mutants at the temperatures at which they do not get significant *Z*-scores are in dotted-line boxes. (C) Z-scores observed at 24 and 26°C of ~5500 deletion strains remaining after the first filtering (see *Materials and Methods*) are plotted. Significant hits (Z-scores > 2.7; *p* values < 0.01) found only at 24°C are shown in green, hits seen only at 26°C in red, and hits found in both screens in yellow. (D–F) Negative interactions found at 24 and 26°C (D and E) and positive ones found at 30°C (F) were manually clustered into functional categories. Functional classes enriched at both 24 and 26°C are in bold. Only interactions remaining after a second filtering (see *Materials and Methods*) are reported.

to 30°C did not destabilize Cdc1-314, although cells depending only on mutant protein do not grow at this temperature (Figure 3A). When cells were shifted to 37°C, a third of Cdc1-314 was degraded within 15–30 min, but the protein remained stable thereafter. The same temperature shifts reduced the amounts of WT Cdc1, but more slowly, so that it took more than 4 h to reach equilibrium levels.

Deletion of the ERAD component *HRD3* increased the amount of WT Cdc1 and Cdc1-314 ~2.3-fold and fourfold, respectively, so Cdc1-314 in *hrd3*Δ is ~1.8-fold more abundant than Cdc1 in *HRD3* cells, at both 30 and 37°C (Figure 4B).

These results suggest that WT Cdc1 is constitutively turned over by ERAD and that the Cdc1-314 is turned over more rapidly than Cdc1 already at 24°C. Moreover, the results strongly suggest that ERAD mutants rescue *cdc1* cells at 30°C through stabilization of Cdc1-314. A similar mechanism may also be invoked for the deletion of *SVP26*, which raises Cdc1-314 levels twofold at 30°C (Figure 4B).

On the other hand, the suppressor effect of *emp24*Δ and *gup1*Δ cannot be explained in terms of Cdc1-314 stability.

Does *cdc1* affect the ER exit of GPI proteins and induce a UPR?

Deletion of *TED1* causes ER retention of Gas1 (Haass *et al.*, 2007) and therewith induces a UPR (Jonikas *et al.*, 2009). We therefore decided to verify whether *cdc1* cells show similar ER retention of GPI proteins and display signs of ER stress. Gas1 is an abundant GPI-anchored β1,3-transglucosidase, which, after extensive *N*- and *O*-glycosylation in the ER, runs with an apparent molecular weight (MW) of 105 kDa on SDS–PAGE, but at 125 kDa after elongation of its glycans in the Golgi (Fankhauser and Conzelmann, 1991). Pulse-chase experiments shown in Figure 5A indicate that *cdc1* cells export Gas1 out of the ER with normal kinetics, whereas its export is delayed in *ted1*Δ mutants. Similarly, as shown by Figure 5B, Western blotting of extracts of *cdc1* cells having been at 24, 30, 33, or 37°C during 4 h show no significant accumulation of an immature ER form of Gas1, much in contrast to *bst1*Δ and *per1*Δ cells (Figure 1). Ccw12 is a GPI-CWP undergoing extensive elongation of its three N-glycans in the Golgi, a process that raises the apparent MW of its 50- and 58-kDa forms to >200 kDa (Ragni *et al.*, 2007). The disappearance of the 50/58-kDa forms of Ccw12 upon addition of cycloheximide was complete within 15 min and followed similar kinetics in *cdc1* and WT cells, indicating that ER-to-Golgi transport and elongation of glycans are not compromised in the *cdc1* mutant (Figure S2).

The accumulation of Gas1 in *per1*Δ and *bst1*Δ cells is also observed in the *cdc1* background, suggesting that the persistence of EtN-P on Man1 does not accelerate ER exit of GPI proteins (Figure S3A).

To measure a potential induction of the UPR, we introduced a multicopy plasmid with the UPR element (UPRE) upstream of lacZ into strains (Menzel *et al.*, 1997). As seen in Figure 5C, *cdc1* showed less UPR activation than WT, at both nonpermissive (30°C) and semipermissive (27°C) temperatures. This, however, was not due to an inability to induce a UPR, since dithiothreitol (DTT) strongly induced lacZ in *cdc1* (Figure 5C).

These results argue that the *cdc1* mutation neither slows nor accelerates the transport of GPI proteins out of the ER.

The reason why *emp24*Δ, *per1*Δ, and *gup1*Δ restore the growth of *cdc1* at 30°C may be that all these mutants reportedly accumulate GPI proteins in the ER (Fujita and Jigami, 2008; Castillon *et al.*, 2011; Figure S3B). This would prolong the time span during which newly synthesized GPI proteins can be acted on by the residual phosphodiesterase activity of Cdc1-314 in the ER, thereby increasing the percentage of correctly processed anchors. It may also be, however,

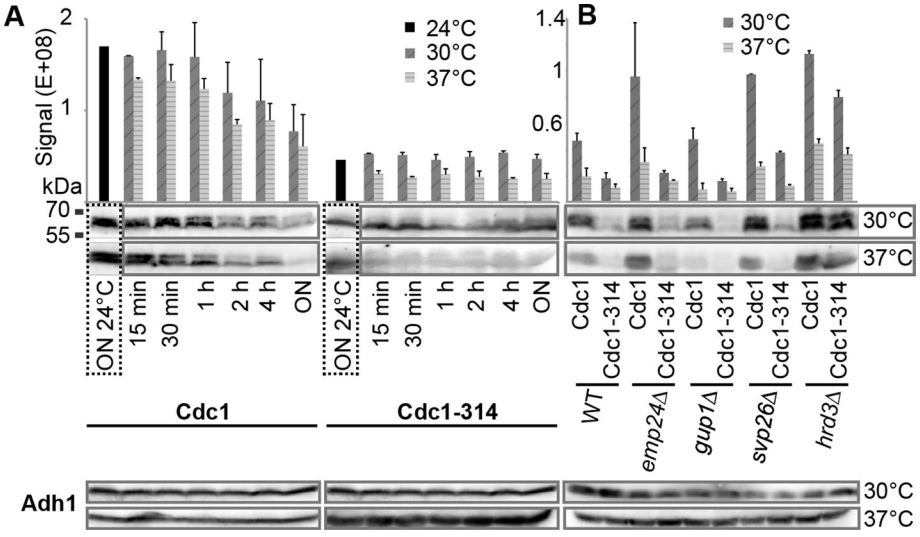

FIGURE 4: Stability of Cdc1-314 and Cdc1 proteins. (A) WT cells harboring HA-tagged Cdc1 or Cdc1-314 proteins were incubated at 24°C overnight (ON) and then shifted to 30 and 37°C for the indicated times. Thereafter cell extracts were subjected to SDS–PAGE and Western blotting using anti-HA antibodies. Adh1 was detected as a loading control. Signals of two biological replicates were averaged and normalized using the Adh1 signals and reference samples (see *Materials and Methods*). (B) Stability of HA-tagged Cdc1 and Cdc1-314 proteins in cells having gene deletions that were identified as suppressors. Cells were incubated overnight at 30 and 37°C before being processed as in A. Quantifications of A and B are not directly comparable, as normalizations were done only within the experiments of each panel.

that the strong UPR induced by deletions such as *emp24*Δ, *per1*Δ, and *gup1*Δ (Jonikas *et al.*, 2009) would help *cdc1* cells to overcome its late secretion block (see Figure 7A later in this article). Indeed, the similar *sec1*^{ts} block is partially cured by a strong UPR (Chang *et al.*, 2004). On the other hand, subsistence of the acyl on the inositol moiety in *bst1*Δ may impede the interaction of the GPI anchor with Cdc1, leading to the strongly negative interaction of *bst1*Δ and *cdc1* (Table S1).

Does *cdc1* affect remodeling of GPI proteins?

In view of the several GPI anchor remodelases that showed either strongly negative (*bst1*Δ) or strongly positive (*per1*Δ, *gup1*Δ) genetic interactions with *cdc1* (Table S2), we wondered whether GPI remodeling was perturbed in *cdc1*. As shown in Figure 5D, detergent-extractable GPI proteins of *cdc1* cells contain a normal amount of ceramide-based, inositol phosphorylceramide (IPC)/B-type anchors. In contrast, *cdc1* cells made three- to fourfold more pG1-type anchors than WT. pG1 is a mild base–sensitive, diacylglycerol-type anchor lipid having C26 in sn2 (Figure 5D). The absolute and relative increase of pG1 raised the possibility that pG1-type GPI anchors are not efficiently transferred from the plasma membrane onto β1,6-glucans, a process, in which the GPI proteins lose the glucosamine–inositol–lipid moiety (Kollar *et al.*, 1997; Fujii *et al.*, 1999).

The profile of the free [^{3}H]inositol-labeled membrane lipids of *cdc1* was normal and showed a normal ratio of mild base–sensitive PI and base-resistant sphingolipids (Figure 5E). However, *cdc1* displayed a consistent relative lack of IPC-C (Figure 5E).

We also labeled *cdc1* cells with [^{14}C]serine, a precursor that labels sphingolipids plus all mature glycerophospholipids, except for PI and mitochondrial lipids. As seen in Figure 5F, the profile of [^{14}C] serine-labeled lipids of *cdc1* cells was normal, whereby a relative reduction of IPCs was noted also by this approach. Apart from the reduction of IPCs, our data are in agreement with a previous report using metabolic labeling with $^{32}PO_4^-$, which concluded that the major sphingo- and phospholipids of the secretory apparatus are unchanged in *cdc1* mutant; still, our method was too crude to detect up-regulation of a minor abnormal phospholipid observed in this previous report (Losev *et al.*, 2008).

Cdc1 cells have fragile cell walls

A previous report showed that growth at 30°C of several *cdc1*^{ts} strains was rescued by osmotic support, but concluded that *CDC1* depletion does not affect cell wall integrity, because 1) *cdc1*^{ts} cells grown with osmotic support at 30°C were not lysed when put into hypotonic media, 2) osmotic support did not rescue growth of *cdc1*^{ts} at 36°C or of *cdc1*Δ, and 3) there were no genetic interactions between *cdc1*^{ts} alleles and genes in the Pkc1-regulated mitogen-activated protein kinase (MAPK) cell integrity pathway (Paidhungat and Garrett, 1998b). The *cdc1-314*^{ts} allele studied here showed the same properties. When kept in YPD in 1 M or 1.4 M sorbitol at 37°C for 24 h, it remained viable (Figure S9) and did not lyse when resuspended thereafter in water (unpublished data); also, our genetic screen failed to show genetic interactions of *cdc1* with the cell wall integrity (CWI) pathway. Yet, as mutants in genes required for cell wall biosynthesis were highly enriched among the negative interactors of *cdc1* (Figure 3, D and E, and Table S2), we nevertheless investigated the susceptibility of *cdc1* to various cell wall–perturbing agents.

As seen in Figure 6A, at 27°C, at which they still grow almost as well as WT, *cdc1* cells were extremely sensitive to very low concentrations of SDS, the N-glycosylation inhibitor tunicamycin, calcofluor white (CFW), and the β1,3-glucan synthase inhibitor caspofungin. Sensitivity to these agents is characteristic for gene mutations affecting cell wall biosynthesis. The extreme tunicamycin hypersensitivity of *cdc1* cannot be due to an inability to induce the UPR (Figure 5C) but may rather be due to the reduced export and functionality of GPI-CWPs and other surface mannoproteins under tunicamycin, an effect that may enhance the cell wall defect of *cdc1*. It should be noted that *bst1*Δ and *per1*Δ single mutants, known to also have cell wall defects, showed no hypersensitivity to the very low concentrations of cell wall–stressing reagents used in Figure 6A. However, as expected from SGA interactions, *cdc1/bst1*Δ were barely growing on YPD (but fully rescued by sorbitol), whereas *cdc1/per1*Δ grew much better than *cdc1* on the cell wall–perturbing agents (Figure 6A), in agreement with the reported rescue of *cdc1-1*^{ts} cells at 30°C by *per1*Δ (= *cos16*Δ) (Paidhungat and Garrett, 1998a) and the data in Figure S1.

As previously discussed, the hypersensitivities to cell wall–perturbing agents are phenotypically suppressed in the *mcd4*Δ background, with the possible exception of the CFW hypersensitivity (Figure 6A, rows *mcd4*Δ and *mcd4*Δ/*cdc1*).

As shown in Figure 6B, growth of *cdc1* cells was normalized by 1 M or 1.4 M sorbitol up to 30 and 35°C, respectively, but not at higher temperatures, and all attempts to generate *cdc1*Δ/*per1*Δ, *cdc1*Δ/*gup1*Δ, *cdc1*Δ/*hrd3*Δ, *cdc1*Δ/*svp26*Δ, or *cdc1*Δ/*emp24*Δ mutants by dissecting tetrads from the corresponding diploid

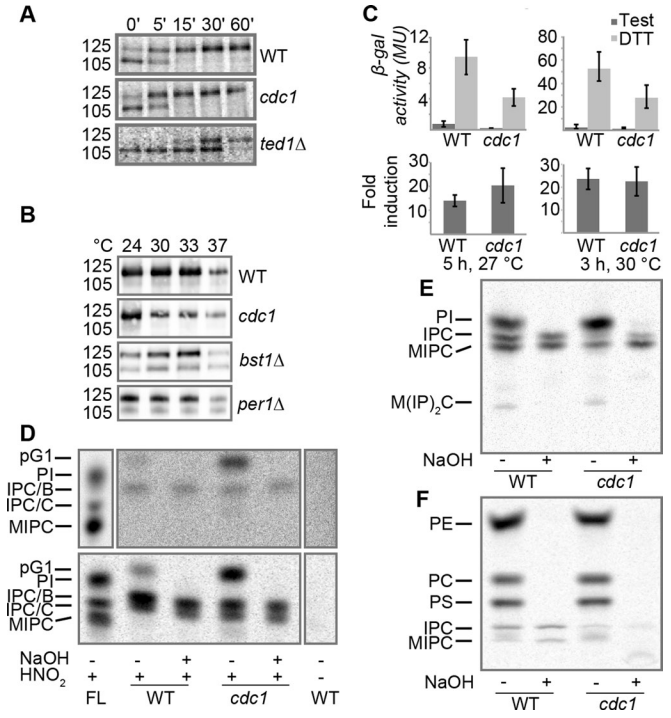

FIGURE 5: Remodeling and export of GPI proteins and induction of UPR in *cdc1*. (A) WT and mutants were pulse labeled with [^{35}S]Met/Cys and chased for indicated times. Gas1 was immunoprecipitated and detected by autoradiography. (B) Western blots using anti-Gas1 antibody of total protein extracts from strains grown for 4 h at 24, 30, 33, or 37°C. (C) WT and *cdc1* carrying an UPRE-lacZ plasmid were preincubated for 5 or 3 h at 27 or 30°C, then further incubated in the presence or absence of DTT for 2 h. Thereafter UPR induction was assessed by measuring β-galactosidase activity, which was plotted as absolute activity (upper plots) or fold induction caused by DTT (lower plots). (D) WT or *cdc1* cells were preincubated at 37°C for 60 min (upper panel) or 10 min (lower panel) and then labeled with [^{3}H]*myo*-inositol for 2 h. Anchor peptides from the total of SDS-extractable GPI proteins were isolated, lipid moieties were released by HNO_2 treatment, subjected or not to mild alkaline deacylation with NaOH, resolved by TLC, and detected by autoradiography. No lipids were seen when HNO_2 treatment was omitted, indicating that only GPI anchor lipids had been isolated. An aliquot of free lipids (FL), not attached to GPI anchors, was run on the same TLC for comparison. (E) Lipid extracts from cells radiolabeled for the upper panel in D were analyzed by TLC and autoradiography before and after deacylation with NaOH. (F) Lipid extracts from [^{14}C]serine-labeled cells preincubated and labeled at 30°C for 5 h were analyzed as in E.

heterozygous double mutants on sorbitol plates failed (unpublished data). The results also suggest that the Cdc1-314 protein is at least partially functional at 35°C, but we cannot be sure that its activity is preserved at 37°C, at which temperature *cdc1* cells, even when having suppressor mutations, stop growing, although the results shown in Figure 4B suggest that cells at 37°C may still have substantial amounts of Cdc1-314 protein.

As shown in Figure 6C, the cell wall defect of *cdc1* cells was discernible even on 1.4 M sorbitol at 32°C when cells were exposed to SDS or tunicamycin. At the same time, they were not hypersensitive to CFW or caspofungin. Thus, although *cdc1* cells maintain at high temperatures a cell wall structure that protects them from subsequent lysis in hypotonic conditions, they are hypersensitive to SDS and tunicamycin, indicating some sort of cell wall abnormality that does not seem to be related to chitin or β1,3-glucan biosynthesis.

Sensitivity of *cdc1* to CFW can be explained by the fact that absolute CFW fluorescence in *cdc1* was much stronger and appeared over the entire cell surface, whereas in WT cells, CFW stained mainly the bud neck and birth scars, as expected (Figure 6D). Occasionally CFW fluorescence was seen at the tip of small buds (Figure 6D, inset), as was also reported for in *dcw1^{ts} dfg5*Δ mutant presumed to be deficient in the transglycosidase anchoring GPI-CWPs in the cell wall (Kitagaki *et al.*, 2004). Lateral chitin depositions are a typical compensation mechanism in mutants having defects in glucan biosynthesis (Popolo *et al.*, 1997; Ram *et al.*, 1998).

On the basis of the extreme hypersensitivity of *cdc1* cells to cell wall–perturbing agents, we propose that *cdc1* cells die at higher temperatures because of a severe cell wall deficiency. This also is supported by the fact that the CWI pathway is activated in *cdc1* cells (Losev *et al.*, 2008). The structure of cell walls in *cdc1* may, however, be quite different from the one in *pkc1* or *rho1* mutants, because only the latter two lyse in hypotonic media after having been on osmotic support (Paidhungat and Garrett, 1998b).

Sorbitol normalizes surface transport of GPI proteins and actin depolarization in *cdc1* cells

The strong negative genetic interaction of *cdc1* with numerous genes required for cell wall biosynthesis (Figure 3, D and E), as well as its hypersensitivity to cell wall–perturbing agents, raised the possibility that *cdc1* cells may have a deficiency in the transport of CWPs later in the secretory apparatus, that is, in the Golgi and beyond. As seen in Figure 7, A and B, when *cdc1* are incubated at 30 or 37°C, the GPI proteins Gas1 and Crh2 accumulate in internal punctate structures. This accumulation is already visible at 27°C (unpublished data). The same punctate structures were also observed for Cwp1 and Cwp2 (Figure S4). When sorbitol was added to media, the intracellular accumulation of GPI proteins was completely relieved (Figures 7A and S4). It appeared conceivable that the intracellular accumulation of GPI proteins in *cdc1* mutants may be related to the loss of actin polarization and actin filaments (Losev *et al.*, 2008), because actin mutants or actin polymerization inhibitor cause a partial block in the late secretory pathway (Novick and Botstein, 1985; Karpova *et al.*, 2000). Similarly, defects in *COF1*, an actin-severing protein, lead to retention of secretory cargo (Bgl2) in the *trans*-Golgi network (Curwin *et al.*, 2012). We therefore tested whether sorbitol can correct actin defects of *cdc1*. As shown in Figure 7, C–E, 1 M sorbitol indeed fully corrected the actin polarization defect at 33°C and did so partially at 37°C.

These data indicate that 1 M sorbitol can rescue the secretion and actin polarization defect. They suggest that the secretion defect of *cdc1* cells may be caused by the perturbation of the actin cytoskeleton (Novick and Botstein, 1985; Karpova *et al.*, 2000), but other data also raise the possibility that the secretion defect is upstream of actin depolarization (Aronov and Gerst, 2004).

Incidentally, the data also confirmed that most *cdc1* cells arrest with small buds when shifted to 33°C, but no longer do so when shifted to 37°C. It has previously been reported that shifts to 30°C arrest cells in G2, but that part of the cells arrest in G1 after a shift to 37°C (Paidhungat and Garrett, 1998b).

Cdc1 establish fewer links between Cwp1 or Cwp2 and cell wall glucans than WT

The fact that sorbitol normalized surface transport of GPI proteins but did not allow growth of cells at 37°C made us believe that GPI proteins of *cdc1* cells retaining an EtN-P on Man1 may not reach their proper destination or may not be properly transferred to the cell wall glucans. After mechanical disruption of yeast cells, the highly cross-linked cell wall glucans remain sedimentable by

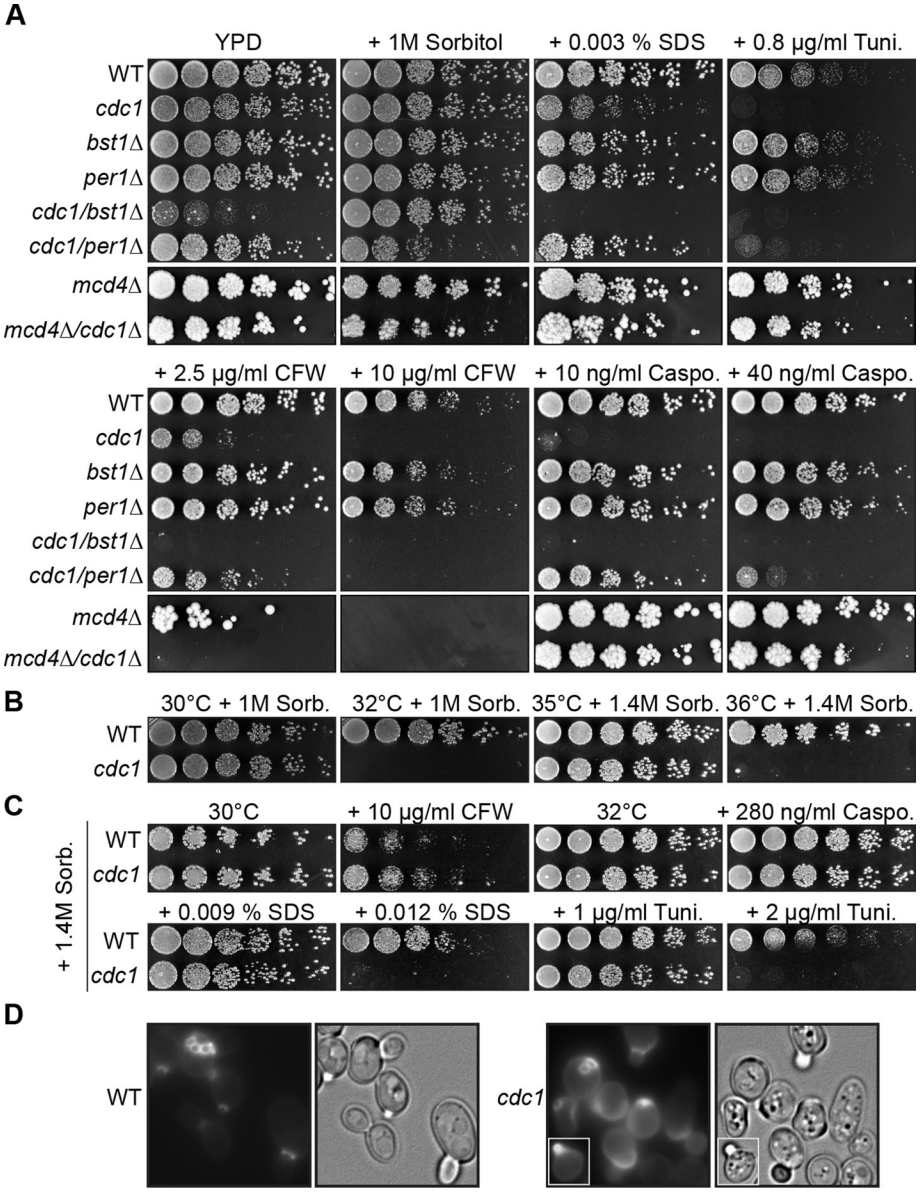

FIGURE 6: *cdc1* cells have fragile cell walls. (A) Fourfold serial dilutions of the indicated strains were spotted onto YPD containing low concentrations of cell wall–perturbing agents and incubated at 30°C (*mcd4*Δ strains) or 27°C (all others). (B) Same as A but plates contained sorbitol (1 or 1.4 M) and were incubated at indicated temperatures. The same picture as in A was also found when the identical assays were repeated on SC medium (unpublished data). (C) WT and *cdc1* were also tested for resistance to cell wall–perturbing agents in the presence of 1.4 M sorbitol, at 30°C for the plate containing CFW and at 32°C for all others. (D) CFW staining of WT and *cdc1* cells grown in YPD at 30°C for 16 h. The pictures are directly comparable, as they were taken using the same exposure time and were processed in the same way. All plates were incubated 2 d except for the ones with *mcd4*Δ strains (4 d).

low-speed centrifugation and are dubbed "cell walls." CWPs are defined as proteins that are not solubilized by boiling cell walls in SDS and 2-mercaptolethanol and remain sedimentable by low-speed centrifugation. Treatment of such SDS-extracted cell walls with linkage-specific glucanases releases proteins such that they no longer sediment with cell walls, enter polyacrylamide gels upon subsequent SDS–PAGE, and can be identified on Western blots (Kapteyn *et al.*, 1995). Classically, CWPs released by β1,6- or β1,3-glucanase are considered to be covalently attached to β1,6- or β1,3-glucans, respectively, whereby the linkage to β1,3-glucans can be either direct via a PIR domain or indirect via β1,6-glucans, which in turn are linked to β1,3-glucans (de Groot *et al.*, 2005). This approach was used to demonstrate that most CWPs are GPI-CWPs, that GPI-CWPs are linked to β1,3-glucans via β1,6-glucans (Kapteyn *et al.*, 1997), and that, in mutants harboring cell wall defects, GPI-CWPs may also be linked (via β1,6-glucans) to chitin (Kapteyn *et al.*, 1997). Moreover, for Cwp1 having a GPI anchor attachment signal and a PIR domain, it was shown that ~40% is doubly linked 1) to β1,6-glucan via the GPI anchor and 2) to β1,3-glucan via a mild base–sensitive linkage involving the PIR domain, the latter linkage becoming more prominent in cells growing at low pH (Kapteyn *et al.*, 2001). This double linkage to both types of β-glucans explains why, in WT cells, part of Cwp1 is neither released by β1,6-glucanase nor base treatment, but only their combination (Kapteyn *et al.*, 2001). Doubly linked GPI-CWPs also may cross-link different β1,3-glucans to each other.

In our experiments done with cells growing in SC medium at low pH (4.2), Cwp1 of WT cells was also released only by combined treatment of β1,3- and β1,6-glucanases and chitinase (Figure 8A, top panel). In contrast, Cwp1 of *cdc1* cells was already released by incubation at 60°C alone, and its release was increased by single digestions with either β1,6- or β1,3-glucanase or chitinase. That higher amounts of Cwp1 are released from *cdc1* cell walls than from WT cell walls is due to the well-known induction of *CWP1* upon cell wall stress (Ram *et al.*, 1998; García *et al.*, 2004; Figure S5). This is apparent also in SDS extracts of cells (Figure 8A, lanes 1–4, top panel).

Cdc1 cells also secreted part of Cwp1 into the culture medium (Figure 8A, lanes 33–36). Secretion of Cwp1 or other CWPs is often observed in mutants having a cell wall defect, such as *gas1*Δ, *gup1*Δ, *per1*Δ, *gpi7*Δ, and *dcw1*^{ts}/*dfg5*Δ (Ram *et al.*, 1998; Kitagaki *et al.*, 2002; Richard *et al.*, 2002; Bosson *et al.*, 2006; Fujita *et al.*, 2006). As shown in Figure S6, the GPI protein Gas1 was also secreted by *cdc1*.

The classical interpretation of the data is to say that most Cwp1 of *cdc1* cells is linked only to either β1,3- or β1,6-glucan or neither, but not both, as is seen in WT cells. Interestingly, the mobility of Cwp1 released from *cdc1* cells by the combination of all glycosidases was slightly lower than the one released from WT cells (Figure 8A, lanes 28–31). This suggested to us that Cwp1 of *cdc1* may have a structure different from the one released from WT.

We also investigated Cwp2, another potentially doubly linked GPI-CWP. *Cdc1*cells expressed less HA-Cwp2 than WT (Figure 8A, lanes 1–4, bottom, and Figure S5). When released from WT cell walls,

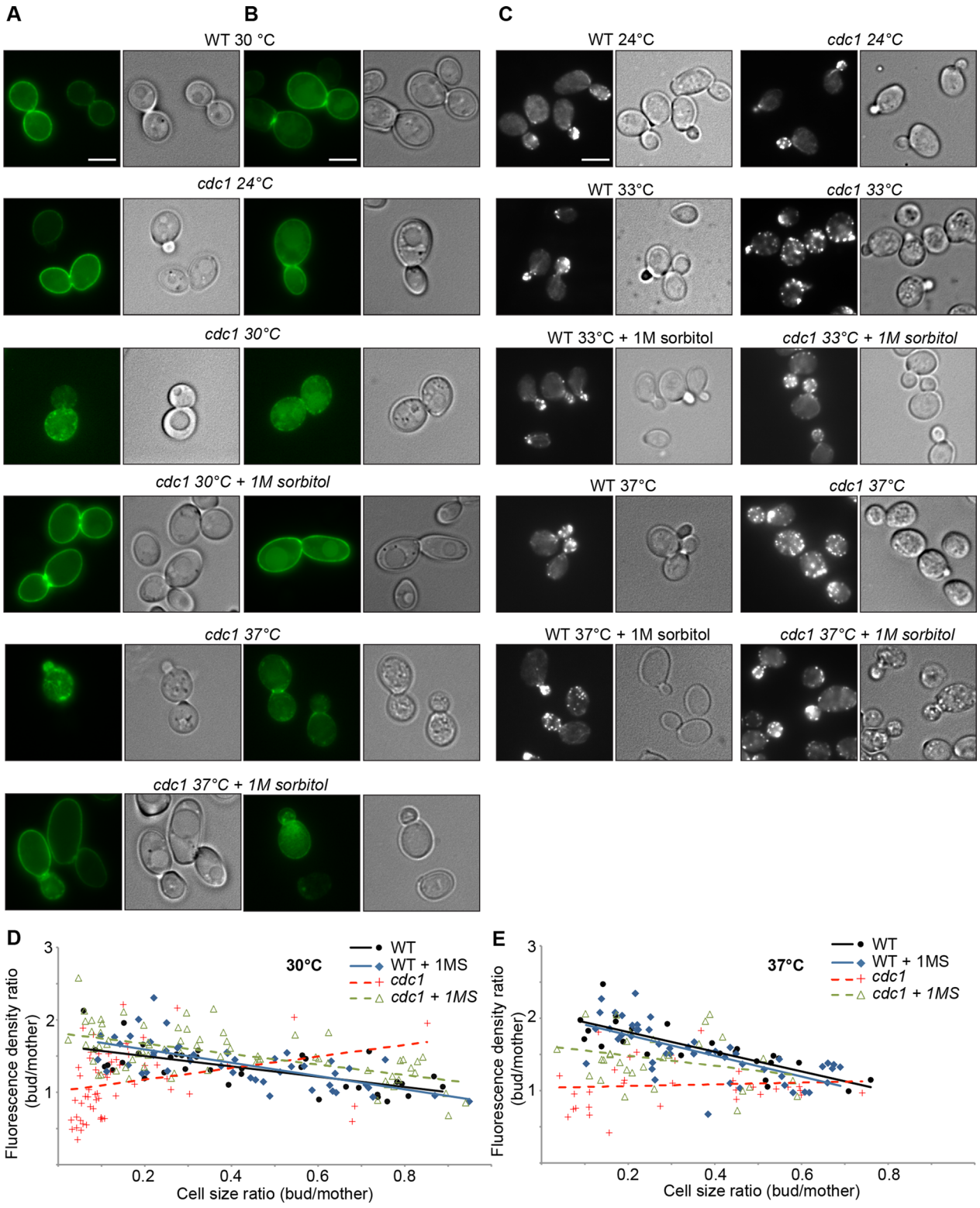

FIGURE 7: Sorbitol normalizes surface transport of GPI proteins and actin depolarization in *cdc1* cells. WT and *cdc1* cells expressing Gas1-GFP (A) or Crh2-GFP (B) under their own promoters and present on centromeric plasmids were grown overnight at the indicated temperatures without or with 1 M sorbitol (+ 1MS). Cells were viewed under a fluorescence microscope. Magnification is the same in all pictures; scale bars: 5 μm. (C) actin patches and cables were stained with rhodamine phalloidin in cells grown overnight under the indicated conditions. (D and E) Actin polarization in cells grown overnight at 33 (D) or 37°C (E) was quantified by measuring the phalloidin fluorescence density in buds and their mothers and then calculating the bud/mother density ratios. Each dot represents a budded cell; bud/mother density ratios are plotted as a function of the bud/mother size ratio and data were subjected to linear regression analysis. Note that these fluorescence density ratios are quite small, because they do not account for the volume but only the area occupied by buds and mothers.

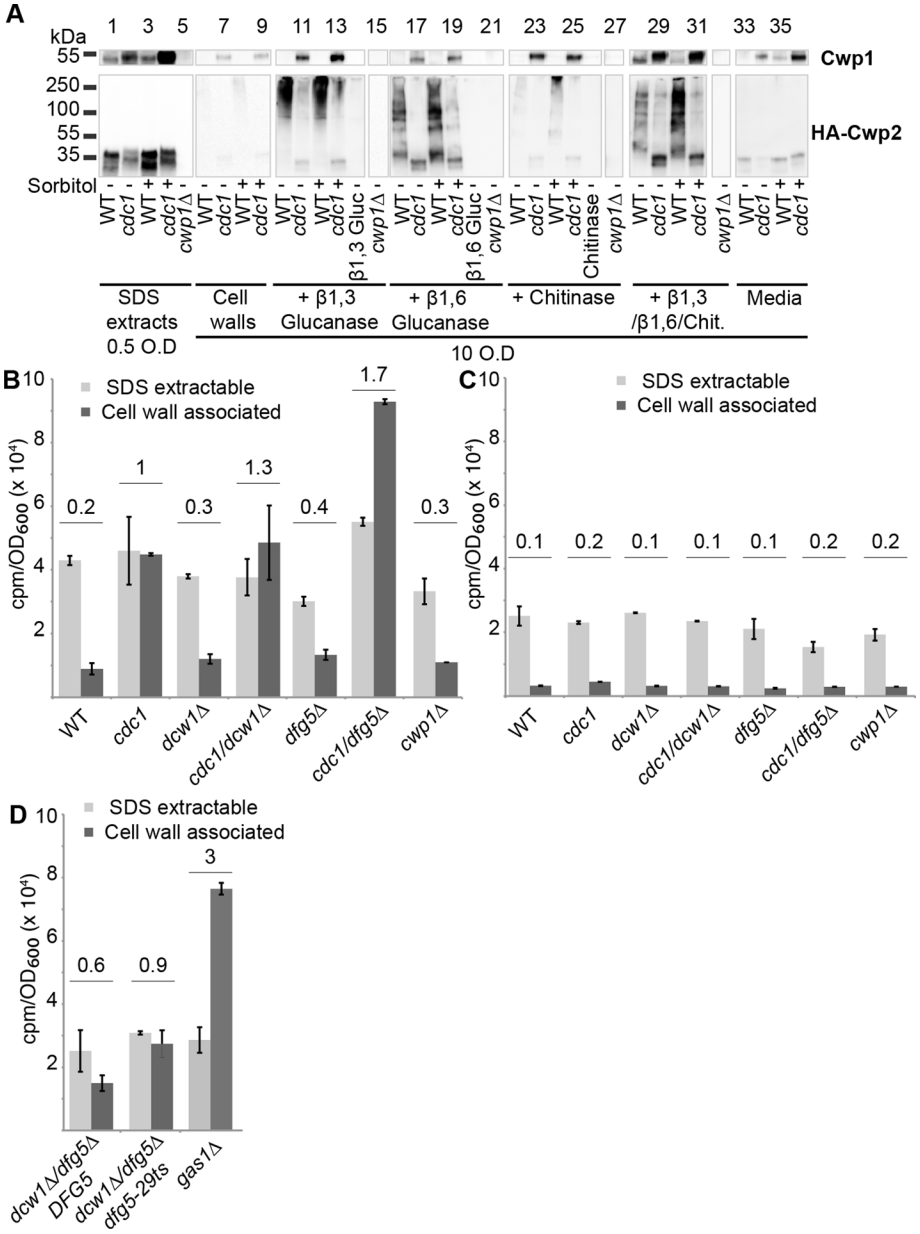

FIGURE 8: The transfer of GPI-CWPs onto β1,6-glucans is compromised in *cdc1* cells. (A) SDS-treated cell walls (10 OD_{600} equivalents) from the indicated strains harboring a plasmid with HA-Cwp2 and having been grown in presence or absence of 1 M sorbitol were digested with the specified glycosidases or control incubated, boiled in sample buffer, and centrifuged. Supernatants were loaded and separated in a 4–20% gradient SDS–PAGE. Cwp1 (top) and HA-Cwp2 (bottom) were detected on Western blots. SDS extracts from the same cells, as well as proteins secreted into the media corresponding to 0.5 and 10 OD_{600} equivalents, respectively, are shown in lanes 1–4 and 33–36. The specificity of the polyclonal anti-Cwp1 antibody is shown in lanes 5, 15, 27, and 32. The antibodies used do not react with the glycosidases used (lanes 14, 20, and 26). (B) Cells of indicated genotypes were metabolically labeled with [^{3}H]*myo*-inositol, mechanically disrupted, and divided into two equal parts. One part was subjected to extensive delipidation using organic solvents, proteins were extracted by repeated boiling in SDS, and nonsoluble material was removed by centrifugation (SDS extractable); in the other part, cell walls were prepared by repeated SDS extraction and were further delipidated with organic solvent (cell wall associated). In both parts, the remaining, GPI protein–associated radioactivity was detected by scintillation counting. (C) Same as in B but cells were grown overnight and labeled in media containing 1 M sorbitol. All strains in B and C, except for *cwp1*Δ, had the Y8205 genetic background. (D) Same as B. Average and SD of three independent experiments and nine measurements are shown for B, and two independent experiments and six measurements are shown for C and D.

HA-Cwp2 appeared as a high-MW smear after β1,3- and as several lower-MW bands (75–200 kDa) after β1,6-glucanase treatment (Figure 8A, lanes 10, 12, 16, and 18). The same lower-MW bands were also observed after combined treatment with all glycosidases (Figure 8A, lanes 28 and 30), although the SDS-soluble HA-Cwp2 runs as a doublet with much lower molecular mass (Figure 8A, lanes 1–4), as described previously (van der Vaart *et al.*, 1996). We assume that the HA-Cwp2 bands running with apparent MWs of 75–200 kDa (Figure 8A, lanes 16, 18, 28, and 30) represent HA-Cwp2 forms with incompletely digested, covalently linked β1,3-glucans, as often observed after β1,3-glucanase (Quantazyme) treatment (Kapteyn *et al.*, 1996). Similarly, the HA-Cwp2 released with β1,6-glucanase may indicate residual attachment to β1,3-glucan. Interestingly, similar to Cwp1, a substantial fraction of HA-Cwp2 was released as a low-MW form from cell walls of *cdc1* cells that had already undergone single digestions with either β1,6-, β1,3-glucanase or chitinase, although combination of all three glycosidases enhanced the recovery (Figure 8A, lanes 11, 13, 17, 19, 23, and 25 vs. lanes 29 and 31). Similar to Cwp1, the smallest form of Cwp2 released from *cdc1* had a slightly different mobility on SDS–PAGE than the one released from WT cell walls, suggesting that these two forms have structurally different C-termini. Part of the HA-Cwp2 released by glucanases from *cdc1* was also running in the 75–200 kDa region (Figure 8A, lanes 11, 13, 17, 19, 29, and 31); this possibly represents HA-Cwp2 that was made before the temperature shift, when cells were growing at 24°C. We therefore used β1,3- and β1,6-glucanases to treat cell walls from *cdc1* cells that were metabolically labeled with [^{35}S]cysteine and [^{35}S]methionine at 37°C. As can be seen in Figure S7, we also found in these experiments that proteins made under restrictive conditions were integrated into the cell wall (in spite of the partial secretion block) and that they could be released through single treatments with β1,6-glucanase.

Proteins may continue to be integrated into the cell wall even under restrictive conditions, either because Cdc1 is not required for this integration process or because the remaining activity of Cdc1-314 at 37°C is sufficient for mere cell wall integration.

Overall the classical interpretation of the data shown in Figure 8A would argue that, in *cdc1* cells, GPI-CWPs continue to be attached via their GPI anchors to β1,6- and β1,3-glucans but that these linkages were established less frequently, as larger than normal proportions of Cwp1 and Cwp2 were released by treatment with only one

enzyme and Cwp2 was recovered as a low-MW form devoid of remaining glucans.

The transfer of GPI-CWPs onto β1,6-glucans is compromised in *cdc1* cells

It seemed possible that the anomalous subsistence of an EtN-P on Man1 in *cdc1* (Figure 1) might interfere with the efficient transfer of GPI-CWPs onto β1,6-glucans. In support of this, we found a strongly negative genetic interaction between *cdc1* and *dfg5*Δ, Dfg5 being one of the supposed transglycosidases that operate this transfer (Kitagaki *et al.*, 2002, 2004).

While the experiments in Figures 8A and S7 suggested that *cdc1* cells continue to covalently add GPI-CWPs to β1,6-glucans, because such proteins can be released from the cell wall by β1,6-glucanase, we considered an alternative interpretation of these results. It seemed conceivable that the dense meshwork of glucans and chitin, possibly rendered thicker and more dense by the cell wall response, would trap GPI proteins still possessing their GPI anchor such that they cannot be released by boiling in SDS and 2-mercaptoethanol, that is, by the classical procedure of preparing cell walls (de Groot *et al.*, 2004). This hypothesis will be referred to as the "trapping model" in the rest of this paper.

We thus sought to test the possibility that proteins not linked covalently to cell walls would be released by β1,6-glucanase simply because this enzyme would render the meshwork of glucans less dense. We tested this by monitoring whether GPI-CWPs remaining in the cell wall fraction after SDS extraction still contain inositol. According to current understanding, this ought not be the case, because the inositol moiety normally is lost when GPI-CWPs are transferred to β1,6-glucans (Figure 1).

As shown in Figure 8B, SDS-extracted GPI proteins of all strains tested contained similar amounts of [^{3}H]inositol, arguing that the incorporation of [^{3}H]inositol into the fraction of free GPI proteins was similar among strains. The same was true for the incorporation of [^{3}H]inositol into lipids (Figure S8). Surprisingly, cell walls of WT cells contained significant amounts of radioactivity (Figure 8B). Moreover, *cdc1-314* mutants contained significantly more cell wall–associated radioactivity than the cell walls of WT, *dcw1*Δ, or *dfg5*Δ mutants. Radioactivity was further increased in cell walls of *cdc1/dfg5*Δ but not of *cdc1/dcw1*Δ cells (Figure 8B).

While the presence of [^{3}H]inositol associated with the SDS-extracted cell walls supports the trapping model, other explanations have to be considered. We can exclude that the cell wall–associated radioactivity is due to the presence of residual free lipids, because all cell wall preparations shown in Figure 8, B–D, after having been extracted four times by boiling in SDS plus 2-mercaptoethanol, were further extracted with chloroform–methanol–water (10:10:3), and these organic solvent extracts did not contain any radioactivity (unpublished data).

We also considered the possibility that radioactivity may be associated with the fraction of Cwp1 that can be released from the cell walls by alkali treatment alone (30% of total; Kapteyn *et al.*, 2001). This fraction of Cwp1 and possibly of three further doubly linkable GPI proteins (Klis *et al.*, 2006), linked only to β1,3-glucans, would retain its [^{3}H]inositol moiety and could therefore account for the radioactivity in cell wall fractions of WT cells. The increase of cell wall–associated radioactivity in *cdc1* cells could thus be the consequence of a cell wall response that induces expression of GPI-CWPs, including doubly linkable GPI-CWPs. However, the absolute amount of cell wall–associated [^{3}H]inositol-containing GPI-CWPs of *cdc1* and *cdc1/dfg5*Δ is comparable to or exceeds the total of SDS-extractable GPI proteins, whereas in WT, protein-associated [^{3}H]inositol in the cell wall fraction is much lower than in the SDS extract. As it is estimated that about half of all GPI proteins remain associated with the plasma membrane (Caro *et al.*, 1997; Hamada *et al.*, 1998; de Groot *et al.*, 2003), the sheer relative amount of [^{3}H]inositol-labeled CWPs in *cdc1* and *cdc1/dfg5*Δ cells makes it rather unlikely that this material would consist merely of the singly linked fraction of doubly linkable GPI-CWPs.

To get further support for the trapping model, we also measured the cell wall–associated [^{3}H]inositol in cell wall mutants such as *gas1*Δ and *cwp1*Δ cells. *Gas1*Δ is extremely CFW hypersensitive, and its cell wall contains 5.3-fold more chitin than WT (Kapteyn *et al.*, 1997), whereas *cwp1*Δ cells are only moderately CFW hypersensitive (van der Vaart *et al.*, 1995). In *gas1*Δ cells the cell walls contain drastically increased amounts of [^{3}H]inositol-labeled GPI-CWPs (Figure 8D), whereas in *cwp1*Δ cells they contain normal amounts (Figure 8B). We also tested the [^{3}H]inositol-labeled GPI-CWPs in cell walls of *dcw1*Δ*/dfg5*Δ cells rescued by either *dfg5-29^{ts}* or *DFG5* (Kitagaki *et al.*, 2004). Mutants rescued by *dfg5-29^{ts}* contained approximately twofold increased levels of [^{3}H]inositol-labeled GPI-CWPs compared with those rescued by *DFG5*, and both strains had higher amounts of labeled proteins in their cell walls than WT (Figure 8D vs. 8B).

Astonishingly, addition of sorbitol to the media totally abolishes the association of [^{3}H]inositol-labeled GPI proteins with the cell wall in mutant and also WT cells (Figure 8C), although the experiments in Figure 8A show that Cwp1 and Cwp2 are still associated with the cell walls of *cdc1* when cells are grown in sorbitol (lanes 13, 19, 25, and 31) and that they can be released by glucanase treatment as low-MW forms, suggesting that they were not connected to residual β-glucans. To explain this paradox, our current working model comprises yet a further type of trapping that would not be relieved by sorbitol and concerns to-be GPI-CWPs having already lost their lipid moiety but being not yet connected to the cell wall glucans. Indeed, it seems conceivable that a first enzyme cleaves the glucosamineα1, 6inositol bond of the GPI anchor (Figure 1) and that the transglycosidation reaction cleaving the Manα1,4glucosamine linkage occurs in a separate, later step. In this scenario, *cdc1* cells may be able to cleave the glucosamineα1,6inositol bond, but not the Manα1,4glucosamine bond, thus leading to a trapping/retention in the cell wall of GPI-CWPs making no covalent bonds to β-glucans but devoid of their lipid anchor.

DISCUSSION

No biochemical defect has so far been identified in *cdc1* cell division–cycle mutants, and it was therefore difficult to make out cause and consequence among the numerous cell biological abnormalities that arise after a temperature upshift in *cdc1^{ts}* mutants. The possible biochemical defect was pinpointed by the groundbreaking study by the Taroh Kinoshita group on PGAP5 (Fujita *et al.*, 2009). Our data indicate that it is likely that the homologous Cdc1 has a function similar to that of PGAP5 and removes EtN-P from Man1 of the GPI anchor, whereas the literature suggests that Ted1 may remove EtN-P from Man2, as does PGAP5. Direct biochemical assays are required to test this hypothesis.

Three main explanations for the strong cell wall phenotype of *cdc1* can be envisaged. Either *cdc1* cells do not transfer GPI-CWPs to the cell wall glucans, because the persistence of EtN-P on Man1 renders the interaction of these proteins with the enzymes operating that transfer less efficient. Indeed, EtN-P is attached to the C2 atom of Man1 (Homans *et al.*, 1988) in the vicinity of the C1 engaged in the glycosidic bond that has to be cleaved in order to transfer Man1 onto β1,6-glucans (Kollar *et al.*, 1997; Fujii *et al.*, 1999). Second, the two presumed transferases Dfg5 and Dcw1 as

well as Gas1, all being GPI proteins themselves, cannot reach the cell surface because of the secretion block that affects the surface transport of GPI proteins in *cdc1* (Figure 7A). From the metabolic labeling studies with [^{32}S]methionine, however, we know that this secretion block is only partial and that as much protein gets into the cell wall of *cdc1* kept at 37°C as in WT (Figure S7). Moreover, cells were grown overnight at 24°C before being labeled at 37°C, and some Dcw1 and Dfg5 made at 24°C ought to still be present at the plasma membrane during the labeling. Thus this second hypothesis seems less likely. Third, the persistence of EtN-P on Man1 leads to mistargeting of GPI-CWPs to inappropriate locations of the cell wall or plasma membrane and thus causes lethality. Also in this scenario, the mislocalization of GPI-CWPs in *cdc1* and the ensuing overproduction of chitin and β-glucans may trap/immobilize Dfg5p, Dcw1, and their substrates, that is, the to-be GPI-CWPs, in a way that they cannot interact. However, the very severe trapping of GPI proteins seen in the perfectly viable *gas1*Δ mutant would argue that at least some types of trapping are not lethal. Of course, it is possible that cell wall–associated [^{3}H]inositol is elevated for different reasons in different mutants, for example, for hypothesis 1 in *cdc1* and for hypothesis 3 in *gas1*Δ.

Discrimination between hypothesis 1 and 3 will require a biochemical in vitro assay of Dcw1 and Dfg5 activities, for which preliminary assays so far have not shown positive results (Hiroshi Kitagaki, personal communication). Whatever the exact reason for the cell wall phenotype of *cdc1*, it currently is not clear whether the failure to remove EtN-P from Man1 concerns all GPI proteins, or only GPI-CWPs, or only a subgroup of them. The major increase in SDS-extractable GPI anchors having the pG1 lipid moiety (Figure 5D) may be an indication that Cdc1 primarily acts on pG1-type GPI anchors. It also could be envisaged that Cdc1 primes certain GPI proteins for transfer into the cell wall by removing the EtN-P from Man1. However, Cdc1 probably acts on more than one GPI protein, because none of the 64 predicted GPI proteins of *Saccharomyces cerevisiae* is essential, but we cannot exclude a dominant effect through which a single unprocessed and mislocalized GPI protein could kill *cdc1* cells.

While Cdc1 may act on only a fraction of GPI proteins, it is clear that all GPI anchors of WT cells initially contain an EtN-P on Man1, because the Gpi10 mannosyltransferase 3 requires this element, as mentioned previously, and the only way to produce GPI anchors lacking EtN-P on Man1 is by way of Cdc1.

Interestingly, the *lack* of EtN-P on Man2 has been invoked as a potential cause for the mistargeting of Egt2, a daughter cell–specific presumed glucanase that is evenly distributed over the bud surface in *gpi7*Δ cells and digests their cell wall, whereas it is directed to the primary septum in WT cells (Fujita *et al.*, 2004). Thus some GPI proteins such as Egt2 may not be acted upon by Ted1, but the inhibitory effect of the *gpi7*Δ deletion on Cwh43-mediated GPI remodeling may also be responsible for this particular sorting defect (Benachour *et al.*, 1999).

Our proposal that *cdc1* cells stop growing at 37°C because of a severe cell wall defect does not exclude the possibility that the growth arrest of *cdc1* at 33°C is due to other reasons, for example, the Ca^{2+} influx, loss of actin filaments, actin polarization, Golgi inheritance (Losev *et al.*, 2008), and/or the partial secretion defect (Figures 7, A and B, and S3). Yet, on sorbitol-containing media, the actin polarization and secretion defects disappear, whereas growth does not resume. Thus severe *CDC1* deficiency leads to a growth defect that cannot be attributed to the actin depolarization and ensuing phenotypes and may be due to the cell wall defect.

*Dcw1*Δ *dfg5*Δ double mutants rescued by a temperature-sensitive allele of either gene arrest after temperature upshift, having small buds, duplicated DNA, nonseparated spindle pole bodies, and depolarized actin cytoskeleton (Kitagaki *et al.*, 2004), a phenotype closely related to *cdc1* mutants (Byers and Goetsch, 1974; Paidhungat and Garrett, 1998b; Losev *et al.*, 2008). Moreover, *dfg5*Δ/*dcw1-3ts* and *dcw1*Δ/*dfg5-29ts* cells could grow at 37°C in 1 M sorbitol, and CFW staining indicated atypical chitin deposition at the tips of small buds (Kitagaki *et al.*, 2004). This similarity argues that *cdc1* mutants may be deficient in the same process that occurs in *dfg5*/*dcw1* mutants, or one that is closely related.

Only *dfg5*Δ, not *dcw1*Δ, shows a negative genetic interaction with *cdc1*, and amounts of [^{3}H]inositol-labeled GPI proteins in cell wall fractions phenocopies the genetic interactions (Figure 8B). One possible reason is that only *DFG5* is induced under cell wall stress (Yoshimoto *et al.*, 2002; Hagen *et al.*, 2004), whereas a similar induction of *DCW1* has not been reported. Alternatively, it may be that GPI proteins having an EtN-P on Man1 are processed only by Dfg5, not Dcw1. Also, the maximal transcription of *DFG5* occurs in G1, while the maximal transcription of *DCW1* occurs in S phase (Kitagaki *et al.*, 2004), and the precise cellular localization of both is currently unknown. It should be noted that some CWPs also tend to be transcribed at different moments in the cell cycle and to locate to different parts of the cell wall (Klis *et al.*, 2006).

The data in Figure 8 led us to propose the somewhat heretical trapping model, which may be especially applicable to mutants having mounted a cell wall response, whereby the trapping of inositol-containing GPI-CWPs is abolished when cells receive osmotic support. A mass spectrometric analysis of yeast CWPs released by mild base or hydrofluoric acid (to cleave the phosphodiester linkage of β1.6-glucan–linked GPI-CWPs) identified 19 CWPs, three of which had neither a GPI attachment signal nor a PIR consensus repeat (Q[IV]XDGQ[IVP]Q; Yin *et al.*, 2005). This supports the idea that, even in WT cells, some CWPs may simply be trapped or be anchored in another yet unknown manner.

MATERIALS AND METHODS

Yeast strains, media, and reagents

Materials were from sources described recently (Ramachandra and Conzelmann, 2013). [^{3}H]*myo*-inositol and [^{14}C]serine were from ARC Radiochemicals (St. Louis, MO); rhodamine phalloidin and Prolong Gold antifade reagent were from Invitrogen. Endo-β1,3-glucanase 81A and endochitinase 18A of *Clostridium thermocellum* were from NZYThec (Lisbon, Portugal); endo-β1,6-glucanase (ThermoActive Pustulanase-Cel 136) was from Prokazyme. Strains, plasmids, and primers used are listed in Supplemental Tables S3–S5. Cells were grown at 30°C on YPD supplemented with uracil and adenine or synthetic complete (SC) medium made from YNB (yeast nitrogen base; United States Biological), supplemented also with amino acids and containing 2% glucose.

Construction of strains and plasmids

Standard methods were used to construct strains for SGA and plasmids with HA- or green fluorescent protein (GFP)-tagged proteins. Detailed procedures are reported in the Supplemental Material.

Protein extraction and quantification

For experiments shown in Figures 4, 5B, S3, and S5, cells were put on ice after addition of 10 mM NaN_3 and NaF. Proteins were extracted (Kushnirov, 2000), separated by SDS–PAGE, and processed for Western blotting, and the immunodetected protein bands were quantified using Image Studio Lite software from LI-COR (Lincoln,

NE). For quantifications of Figure 4, the anti-HA signal of each lane was first normalized using Adh1 to correct small errors of protein loading during SDS–PAGE. All gels for the experiments in a given panel (A or B) contained a reference sample that was used to normalize and compare the values between different gels. The doubly normalized data were then used to get a mean and SD for each condition.

Measuring β-galactosidase activity

Assays were done as described by Guarente (1983) but with the modifications described in the Supplemental Material.

Pulse-chase metabolic labeling of proteins using [^{35}S] methionine/cysteine

Pulse-chase experiments were done as previously described (Watanabe *et al.*, 2002) with the modifications described in the Supplemental Material.

Metabolic labeling of cells with [^{3}H]*myo*-inositol or [^{14}C] serine

For labeling with [^{3}H]*myo*-inositol (Figures 5, D and E, and 8, B–D), cells were grown to exponential phase at 24°C in inositol-free SC medium containing or not 1 M sorbitol. Ten OD_{600} were collected, resuspended in 1 ml fresh medium of the same kind, and preincubated at 37°C for 10 or 60 min in a water bath with good aeration (shaking). At $t = 0$, 40 μCi of [^{3}H]*myo*-inositol was added. Fresh medium (0.2 ml) from a 5× concentrated stock was added at $t = 0$, 40, and 80 min if cells had been preincubated for 60 min, and at $t = 40$ and 80 min if they had been preincubated for 10 min. Labeling was stopped after 2 h. GPI anchor lipids and free lipids (Figure 5, D and E) were isolated and analyzed as described by Guillas *et al.* (2000). Free lipids were migrated on TLC silica plates in chloroform–methanol–water (10:10:2.5), and anchor lipids were migrated in chloroform–methanol–0.25% KCl (55:45:10) solvent systems. GPI proteins (Figure 8, B–D) and lipids (Figure S8) to be used for scintillation counting were extracted from labeled cells as described for analysis of anchor lipids (Guillas *et al.*, 2000), that is, by breaking cells with glass beads in organic solvent, but delipidated protein pellets were incubated with ethanol–water–diethyl ether–pyridine–ammonia (15:15:5:1:0.018 vol/vol) at 60°C for 15 min, dried down, and further extracted with chloroform–methanol–water (10:10:2.5) to remove residual lipids. Final protein pellets containing labeled GPI proteins were solubilized by boiling them twice for 10 min in counting buffer (2% SDS, 5% 2-mercaptoethanol) and counted in a scintillation counter.

For labeling with [^{14}C]serine (Figure 5F), cells were grown to exponential phase at 24°C in YPD. Three OD_{600} were collected, washed, and resuspended in 3 ml serine-free SC medium. Cells were then labeled with 3 μCi of [^{14}C]serine in a shaking water bath at 30°C for 5 h. Thereafter equivalent numbers of OD_{600} units of cells were collected from all strains, and lipids were extracted as described by Guan *et al.* (2010) but no standards were used. Lipids were separated on TLC silica plates in chloroform–methanol–4.2 N ammonia (9:7:2) solvent system.

Mild base treatment of lipids

Dried lipids were resuspended in 200 μl chloroform–methanol–water (10:10:3), 40 μl of 0.6 M NaOH in methanol was added, and samples were incubated at 37°C for 1 h. Hydrolysis was stopped with 40 μl of 0.8 M acetic acid, and the lipids were dried. Control samples followed the same procedure, but NaOH and acetic acid were added together at the end of the incubation. Dried lipids were desalted by butanol–water partitioning as described by Guillas *et al.* (2000).

Fluorescence microscopy

Fluorescence microscopy was done using an Olympus BX51 microscope. Detailed procedures are contained in the Supplemental Material.

Cell wall isolation and protein extraction

Cell walls (Figures 8 and S7) were isolated as described by de Groot *et al.* (2004) but with the following modifications: cells were lysed with glass beads in 50 mM Tris-HCl (pH 7.5) containing 1 mM EDTA, 1 μM pepstatin, 1 mM phenylmethylsulfonyl fluoride, and Roche protease inhibitor cocktail. After lysis, SDS, NaCl, and β-mercaptoethanol were added to final concentrations of 4%, 100 mM, and 40 mM, respectively, and lysates were boiled for 10 min. Boiled lysates were centrifuged (16,000 × *g*, 5 min) and the pellets were extracted three more times by each time adding fresh extraction buffer (4% SDS, 100 mM NaCl and 40 mM β-mercaptoethanol), boiling for 2 min, and centrifuging. After having been extracted four times, the resulting cell walls were washed three times with water and used directly for glycosidase digestions. Cell walls corresponding to 50 OD_{600} units of cells were digested in 100 μl of 100 mM sodium phosphate (pH 6) with 0.2 U/μl of endo-β1,3-glucanase 81A, 0.05 U/μl of endo-β1,6-glucanase, and/or 0.0025 U/μl of endochitinase 18A. The buffer of the glycosidases was changed to 100 mM sodium phosphate (pH 6) using Vivaspin columns with a 10-kDa cutoff before being added to cell walls. All samples were first incubated for 5 h at 60°C, which is the optimal temperature for β1,3-glucanase and chitinase, then 5 h at 80°C, the optimal temperature for β1,6-glucanase. After the incubations, SDS sample buffer (60 mM Tris-HCl, pH 6.8, 3.3% SDS, 5% glycerol, 100 mM DTT, and 3 mM bromphenol blue) was added and samples were boiled for 10 min and centrifuged 5 min at 16,000 × *g*. Extracted proteins were resolved in 4–20% gradient SDS–PAGE and transferred to PVDF membranes. HA-Cwp2 was detected using anti-HA antibodies, Cwp1 and Gas1 were detected using specific antibodies against these proteins.

For detection of radiolabeled GPI proteins associated with the cell wall, SDS-treated cell walls (see preceding paragraph) from cells labeled with [^{3}H]*myo*-inositol were washed three times with water and further delipidated two times with 500 μl chloroform–methanol–water (10:10:3), resuspended in counting buffer (2% SDS, 5% 2-mercaptoethanol), and boiled for 10 min before scintillation counting.

Precipitation of proteins in culture media

Culture media corresponding to 30 OD_{600} were concentrated down to 1.2 ml using Vivaspin columns with a cutoff of 10 kDa. Five micrograms of bovine serum albumin was added, and proteins were precipitated by adding 300 μl 100% trichloroacetic acid (20% final concentration) and incubated for 40 min at −20°C. Pellets were rinsed twice with ethanol/Tris-HCl, pH 8.8, dried, resuspended in SDS sample buffer, and boiled for 10 min.

ACKNOWLEDGMENTS

We thank Javier Arroyo, Charlie Boone, Brendan Cormack, Benjamin Glick, Hiroshi Kitagaki, Frans Klis, Laura Popolo, and Sabine Strahl-Bolsinger for strains, antibodies, and plasmids; and Manuel Muñiz, Frans Klis, and Hiroshi Kitagaki for helpful information. This work was supported by grants CRSI33_125232 and 31003AB_131078 from the Swiss National Science Foundation.

REFERENCES

Aronov S, Gerst JE (2004). Involvement of the late secretory pathway in actin regulation and mRNA transport in yeast. J Biol Chem 279, 36962–36971.

Benachour A, Sipos G, Flury I, Reggiori F, Canivenc-Gansel E, Vionnet C, Conzelmann A, Benghezal M (1999). Deletion of GPI7, a yeast gene required for addition of a side chain to the glycosylphosphatidylinositol (GPI) core structure, affects GPI protein transport, remodeling, and cell wall integrity. J Biol Chem 274, 15251–15261.

Bosson R, Jaquenoud M, Conzelmann A (2006). GUP1 of *Saccharomyces cerevisiae* encodes an *O*-acyltransferase involved in remodeling of the GPI anchor. Mol Biol Cell 17, 2636–2645.

Breslow DK, Cameron DM, Collins SR, Schuldiner M, Stewart-Ornstein J, Newman HW, Braun S, Madhani HD, Krogan NJ, Weissman JS (2008). A comprehensive strategy enabling high-resolution functional analysis of the yeast genome. Nat Methods 5, 711–718.

Byers B, Goetsch L (1974). Duplication of spindle plaques and integration of the yeast cell cycle. Cold Spring Harb Symp Quant Biol 38, 123–131.

Caro LH, Tettelin H, Vossen JH, Ram AF, Van Den Ende H, Klis FM (1997). In silicio identification of glycosyl-phosphatidylinositol-anchored plasma-membrane and cell wall proteins of *Saccharomyces cerevisiae*. Yeast 13, 1477–1489.

Castillon GA, Aguilera-Romero A, Manzano-Lopez J, Epstein S, Kajiwara K, Funato K, Watanabe R, Riezman H, Muniz M (2011). The yeast p24 complex regulates GPI-anchored protein transport and quality control by monitoring anchor remodeling. Mol Biol Cell 22, 2924–2936.

Castillon GA, Watanabe R, Taylor M, Schwabe TME, Riezman H (2009). Concentration of GPI-anchored proteins upon ER exit in yeast. Traffic 10, 186–200.

Chang HJ, Jesch SA, Gaspar ML, Henry SA (2004). Role of the unfolded protein response pathway in secretory stress and regulation of INO1 expression in *Saccharomyces cerevisiae*. Genetics 168, 1899–1913.

Curwin AJ, von Blume J, Malhotra V (2012). Cofilin-mediated sorting and export of specific cargo from the Golgi apparatus in yeast. Mol Biol Cell 23, 2327–2338.

de Groot PWJ, de Boer AD, Cunningham J, Dekker HL, de Jong L, Hellingwerf KJ, de Koster C, Klis FM (2004). Proteomic analysis of *Candida albicans* cell walls reveals covalently bound carbohydrate-active enzymes and adhesins. Eukaryotic Cell 3, 955–965.

de Groot PWJ, Hellingwerf KJ, Klis FM (2003). Genome-wide identification of fungal GPI proteins. Yeast 20, 781–796.

de Groot PWJ, Ram AF, Klis FM (2005). Features and functions of covalently linked proteins in fungal cell walls. Fungal Genet Biol 42, 657–675.

Eguez L, Chung Y-S, Kuchibhatla A, Paidhungat M, Garrett S (2004). Yeast Mn^{2+} transporter, Smf1p, is regulated by ubiquitin-dependent vacuolar protein sorting. Genetics 167, 107–117.

Fankhauser C, Conzelmann A (1991). Purification, biosynthesis and cellular localization of a major 125-kDa glycophosphatidylinositol-anchored membrane glycoprotein of *Saccharomyces cerevisiae*. Eur J Biochem 195, 439–448.

Fankhauser C, Homans SW, Thomas-Oates JE, McConville MJ, Desponds C, Conzelmann A, Ferguson MA (1993). Structures of glycosylphosphatidylinositol membrane anchors from *Saccharomyces cerevisiae*. J Biol Chem 268, 26365–26374.

Fujii T, Shimoi H, Iimura Y (1999). Structure of the glucan-binding sugar chain of Tip1p, a cell wall protein of *Saccharomyces cerevisiae*. Biochim Biophys Acta 1427, 133–144.

Fujita M, Jigami Y (2008). Lipid remodeling of GPI-anchored proteins and its function. Biochim Biophys Acta 1780, 410–420.

Fujita M, Maeda Y, Ra M, Yamaguchi Y, Taguchi R, Kinoshita T (2009). GPI glycan remodeling by PGAP5 regulates transport of GPI-anchored proteins from the ER to the Golgi. Cell 139, 352–365.

Fujita M, Yoko-O T, Jigami Y (2006). Inositol deacylation by Bst1p is required for the quality control of glycosylphosphatidylinositol-anchored proteins. Mol Biol Cell 17, 834–850.

Fujita M, Yoko-O T, Okamoto M, Jigami Y (2004). GPI7 involved in glycosylphosphatidylinositol biosynthesis is essential for yeast cell separation. J Biol Chem 279, 51869–51879.

García R, Bermejo C, Grau C, Pérez R, Rodríguez-Peña JM, François J, Nombela C, Arroyo J (2004). The global transcriptional response to transient cell wall damage in *Saccharomyces cerevisiae* and its regulation by the cell integrity signaling pathway. J Biol Chem 279, 15183–15195.

Guan XL, Riezman I, Wenk MR, Riezman H (2010). Yeast lipid analysis and quantification by mass spectrometry. Methods Enzymol 470, 369–391.

Guarente L (1983). Yeast promoters and lacZ fusions designed to study expression of cloned genes in yeast. Methods Enzymol 101, 181–191.

Guillas I, Pfefferli M, Conzelmann A (2000). Analysis of ceramides present in glycosylphosphatidylinositol anchored proteins of *Saccharomyces cerevisiae*. Methods Enzymol 312, 506–515.

Haass FA, Jonikas M, Walter P, Weissman JS, Jan Y-N, Jan LY, Schuldiner M (2007). Identification of yeast proteins necessary for cell-surface function of a potassium channel. Proc Natl Acad Sci USA 104, 18079–18084.

Hagen I, Ecker M, Lagorce A, Francois JM, Sestak S, Rachel R, Grossmann G, Hauser NC, Hoheisel JD, Tanner W, Strahl S (2004). Sed1p and Srl1p are required to compensate for cell wall instability in *Saccharomyces cerevisiae* mutants defective in multiple GPI-anchored mannoproteins. Mol Microbiol 52, 1413–1425.

Hamada K, Fukuchi S, Arisawa M, Baba M, Kitada K (1998). Screening for glycosylphosphatidylinositol (GPI)-dependent cell wall proteins in *Saccharomyces cerevisiae*. Mol Gen Genet 258, 53–59.

Homans SW, Ferguson MA, Dwek RA, Rademacher TW, Anand R, Williams AF (1988). Complete structure of the glycosyl phosphatidylinositol membrane anchor of rat brain Thy-1 glycoprotein. Nature 333, 269–272.

Jonikas MC, Collins SR, Denic V, Eugene O, Quan EM, Schmid V, Weibezahn J, Schwappach B, Walter P, Weissman JS, Schuldiner M (2009). Comprehensive characterization of genes required for protein folding in the endoplasmic reticulum. Science 323, 1693–1697.

Kapteyn JC, Montijin RC, Vink E, la Cruz de J, Llobell A, Douwes JE, Shimoi H, Lipke PN, Klis FM (1996). Retention of *Saccharomyces cerevisiae* cell wall proteins through a phosphodiester-linked β-1,3-/β-l,6-glucan heteropolymer. Glycobiology 6, 337–345.

Kapteyn JCJ, Montijn RCR, Dijkgraaf GJG, Van Den Ende HH, Klis FMF (1995). Covalent association of beta-1,3-glucan with beta-1,6-glucosylated mannoproteins in cell walls of *Candida albicans*. J Bacteriol 177, 3788–3792.

Kapteyn JCJ, Ram AFA, Groos EME, Kollar RR, Montijn RCR, Van Den Ende HH, Llobell AA, Cabib EE, Klis FMF (1997). Altered extent of cross-linking of beta1,6-glucosylated mannoproteins to chitin in *Saccharomyces cerevisiae* mutants with reduced cell wall beta1,3-glucan content. J Bacteriol 179, 6279–6284.

Kapteyn JC, Riet Ter B, Vink E, Blad S, De Nobel H, Van Den Ende H, Klis FM (2001). Low external pH induces HOG1-dependent changes in the organization of the *Saccharomyces cerevisiae* cell wall. Mol Microbiol 39, 469–479.

Karpova TS, Reck-Peterson SL, Elkind NB, Mooseker MS, Novick PJ, Cooper JA (2000). Role of actin and Myo2p in polarized secretion and growth of *Saccharomyces cerevisiae*. Mol Biol Cell 11, 1727–1737.

Kitagaki H, Ito K, Shimoi H (2004). A temperature-sensitive dcw1 mutant of *Saccharomyces cerevisiae* is cell cycle arrested with small buds which have aberrant cell walls. Eukaryotic Cell 3, 1297–1306.

Kitagaki H, Wu H, Shimoi H, Ito K (2002). Two homologous genes, DCW1 (YKL046c) and DFG5, are essential for cell growth and encode glycosylphosphatidylinositol (GPI)-anchored membrane proteins required for cell wall biogenesis in *Saccharomyces cerevisiae*. Mol Microbiol 46, 1011–1022.

Klis FM, Boorsma A, de Groot PWJ (2006). Cell wall construction in *Saccharomyces cerevisiae*. Yeast 23, 185–202.

Kollar RR, Reinhold BBB, Petráková EE, Yeh HJH, Ashwell GG, Drgonová JJ, Kapteyn JCJ, Klis FMF, Cabib EE (1997). Architecture of the yeast cell wall. Beta(1→6)-glucan interconnects mannoprotein, beta(1→3)-glucan, and chitin. J Biol Chem 272, 17762–17775.

Kushnirov VV (2000). Rapid and reliable protein extraction from yeast. Yeast 16, 857–860.

Losev E, Papanikou E, Rossanese OW, Glick BS (2008). Cdc1p is an endoplasmic reticulum-localized putative lipid phosphatase that affects Golgi inheritance and actin polarization by activating Ca^{2+} signaling. Mol Cell Biol 28, 3336–3343.

Loukin S, Kung C (1995). Manganese effectively supports yeast cell-cycle progression in place of calcium. J Cell Biol 131, 1025–1037.

Maeda Y, Kinoshita T (2011). Structural remodeling, trafficking and functions of glycosylphosphatidylinositol-anchored proteins. Prog Lipid Res 50, 411–424.

Menzel R, Vogel F, Kärgel E, Schunck WH (1997). Inducible membranes in yeast: relation to the unfolded-protein-response pathway. Yeast 13, 1211–1229.

Novick P, Botstein D (1985). Phenotypic analysis of temperature-sensitive yeast actin mutants. Cell 40, 405–416.

Paidhungat M, Garrett S (1997). A homolog of mammalian, voltage-gated calcium channels mediates yeast pheromone-stimulated Ca^{2+} uptake and exacerbates the cdc1(Ts) growth defect. Mol Cell Biol 17, 6339–6347.

Paidhungat MM, Garrett SS (1998a). Cdc1 and the vacuole coordinately regulate Mn^{2+} homeostasis in the yeast *Saccharomyces cerevisiae*. Genetics 148, 1787–1798.

Paidhungat M, Garrett S (1998b). Cdc1 is required for growth and Mn^{2+} regulation in *Saccharomyces cerevisiae*. Genetics 148, 1777–1786.
Pittet M, Conzelmann A (2007). Biosynthesis and function of GPI proteins in the yeast *Saccharomyces cerevisiae*. Biochim Biophys Acta 1771, 405–420.
Popolo L, Gilardelli D, Bonfante P, Vai M (1997). Increase in chitin as an essential response to defects in assembly of cell wall polymers in the gg-p1delta mutant of *Saccharomyces cerevisiae*. J Bacteriol 179, 463–469.
Ragni E, Sipiczki M, Strahl S (2007). Characterization of Ccw12p, a major key player in cell wall stability of *Saccharomyces cerevisiae*. Yeast 24, 309–319.
Ram AF, Kapteyn JC, Montijn RC, Caro LH, Douwes JE, Baginsky W, Mazur P, Van Den Ende H, Klis FM (1998). Loss of the plasma membrane-bound protein Gas1p in *Saccharomyces cerevisiae* results in the release of beta1,3-glucan into the medium and induces a compensation mechanism to ensure cell wall integrity. J Bacteriol 180, 1418–1424.
Ramachandra N, Conzelmann A (2013). Membrane topology of yeast alkaline ceramidase YPC1. Biochem J 452, 585–594.
Richard MM, De Groot PP, Courtin OO, Poulain DD, Klis FF, Gaillardin CC (2002). GPI7 affects cell-wall protein anchorage in *Saccharomyces cerevisiae* and *Candida albicans*. Annu Rev Microbiol 148, 2125–2133.
Rossanese OW, Reinke CA, Bevis BJ, Hammond AT, Sears IB, O'Connor J, Glick BS (2001). A role for actin, Cdc1p, and Myo2p in the inheritance of late Golgi elements in *Saccharomyces cerevisiae*. J Cell Biol 153, 47–62.
Supek F, Supekova L, Nelson H, Nelson N (1996). A yeast manganese transporter related to the macrophage protein involved in conferring resistance to mycobacteria. Proc Natl Acad Sci USA 93, 5105–5110.
van der Vaart JM, Caro LH, Chapman JW, Klis FM, Verrips CT (1995). Identification of three mannoproteins in the cell wall of *Saccharomyces cerevisiae*. J Bacteriol 177, 3104–3110.
van der Vaart JM, van Schagen FS, Mooren AT, Chapman JW, Klis FM, Verrips CT (1996). The retention mechanism of cell wall proteins in *Saccharomyces cerevisiae*. Wall-bound Cwp2p is beta-1,6-glucosylated. Biochim Biophys Acta 1291, 206–214.
Watanabe R, Funato K, Venkataraman K, Futerman AH, Riezman H (2002). Sphingolipids are required for the stable membrane association of glycosylphosphatidylinositol-anchored proteins in yeast. J Biol Chem 277, 49538–49544.
Yin QY, de Groot PWJ, Dekker HL, de Jong L, Klis FM, De Koster CG (2005). Comprehensive proteomic analysis of Saccharomyces cerevisiae cell walls: identification of proteins covalently attached via glycosylphosphatidylinositol remnants or mild alkali-sensitive linkages. J Biol Chem 280, 20894–20901.
Yoshimoto H, Saltsman K, Gasch AP, Li HX, Ogawa N, Botstein D, Brown PO, Cyert MS (2002). Genome-wide analysis of gene expression regulated by the calcineurin/Crz1p signaling pathway in *Saccharomyces cerevisiae*. J Biol Chem 277, 31079–31088.
Zhu Y, Vionnet C, Conzelmann A (2006). Ethanolaminephosphate side chain added to glycosylphosphatidylinositol (GPI) anchor by mcd4p is required for ceramide remodeling and forward transport of GPI proteins from endoplasmic reticulum to Golgi. J Biol Chem 281, 19830–19839.